AiMT Advances in Military Technology
Vol. 8, No. 1, June 2013

Apertures with Laval Nozzle and Circular Orifice in Secondary Electron Detector for Environmental Scanning Electron Microscope

P. Vyroubal[1], J. Maxa[1*], V. Neděla[2], J. Jirák[1,2] and K. Hladká[1]

[1] *Department of Electrical and Electronic Technology, Faculty of Electrical Engineering and Communication, Brno University of Technology, Czech Republic*
[2] *Institute of Scientific Instruments of the ASCR, v.v.i., Brno, Czech Republic*

The manuscript was received on 18 January 2013 and was accepted after revision for publication on 20 March 2013.

Abstract:

Environmental scanning electron microscopes offer wide possibilities for the exploration of various types of specimens, especially non-conductive and wet specimens containing different material phases. The evaluation of pressure on the secondary electrons trajectory is one of the important parameters in design of scintillation detector of secondary electrons. The final process is influenced by the size and the shape of the apertures used to separate areas with different pressure gradient. This article is focused on the comparison of the aperture with circular orifice and aperture with Laval nozzle. .

Keywords:

Aperture, Laval nozzle, circular orifice, pressure, detector, Mach number, flow, trajectory of secondary electrons.

1. Introduction

Scintillation and ionization detectors are used to detect secondary electrons. The ionization detector works on the principle of impact ionization. The scintillation detector contains a scintillator (e.g. YAG, CRY 18, etc.) which releases electrons when they hit a flash of light whose intensity is proportional to the energy of incident electrons [1].

The scintillator in the scintillation detector of secondary electrons is placed in a separately pumped chamber separated from the specimen chamber by apertures C1 and C2 (Fig. 1). Electric potential of hundreds of volts is applied on the apertures.

[*] *Corresponding author: Department of Electrical and Electronic Technology, Faculty of Electrical Engineering and Communication, Brno University of Technology, Technická 10, 616 00 Brno, Czech Republic, phone: +420 54114 6129, E-mail: maxa@feec.vutbr.cz*

Apertures form electrostatic lens. Secondary electrons are directed by the electrodes to the lens in the mouth of the detector and then the electrons pass through it. Apertures also prevent gas flow from the sample chamber into the scintillator chamber. In the specimen chamber there is a gas pressure from 0.01 to 1,000 Pa.

At the maximum pressure of 5 Pa in the scintillator chamber, a voltage up to 8 kV can be attached to the scintillator without causing a gas discharge. This voltage accelerates the electrons through the apertures with an energy which is sufficient to generate scintillation. Photons created by scintillation are kept in the light guide into photomultiplier, where they are amplified and converted into an electrical signal [2].

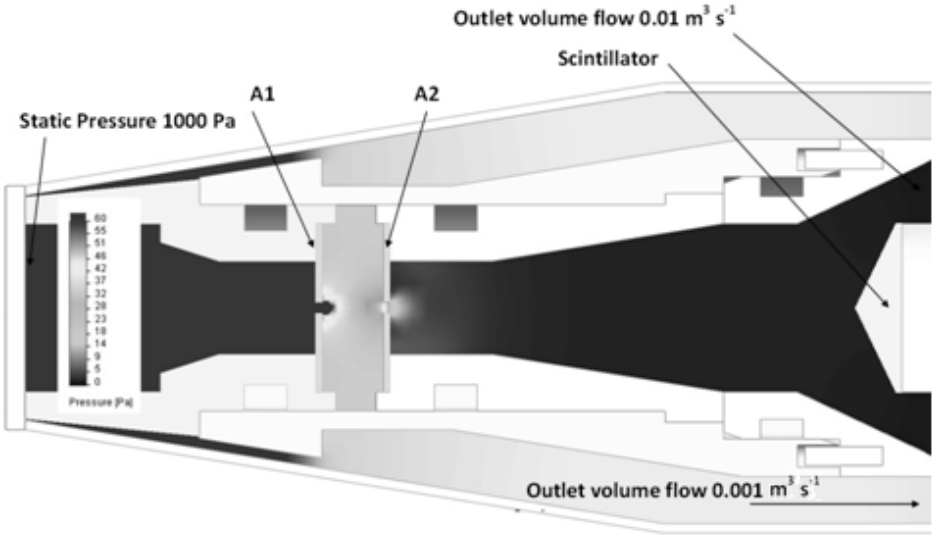

Fig. 1 Functional scheme of the scintillation detector of secondary electrons

The orifices of small dimensions are found in the construction of the electron microscope, where it is necessary to separate areas with a large pressure gradient without the possibility of perfect isolation (Fig. 2). The pressure in the fluid flow depends on the speed of flow. The higher the speed is, the lower gas pressure can be achieved by reducing the size of the orifice in apertures or changing their shape [3-5]. In terms of detectors, the following aspects are important:

1. The pressure in the area of a scintillation crystal must be higher than 5 Pa to avoid electric discharge in the gas because of the high voltage on the scintillator (up to 8 kV).
2. Average pressure on the trajectory of secondary electrons must be low to avoid scattering of electrons.

2. Mathematical Interpretation

For the modelling of individual apertures, the SolidWorks detector and SolidWorks Flow Simulation were used and thus the flow can be calculated using the finite volumes method. Flow Simulation solves a system of three partial differential equations, completed with a fourth equation of state. It is a type of three-dimensional flow of compressible viscous fluid. Basic equations describing the flow of viscous

compressible fluid written in conservative form are three conservation laws, law of conservation of mass, momentum and energy completed with the fourth equation of state of the considered fluid [6].

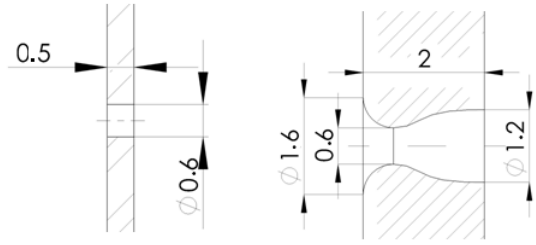

Fig. 2 Illustration of the detector and investigated apertures in Flow Simulation

Continuity equation (1) expresses the law of conservation of mass and it takes the form

$$\frac{\partial \rho_{\mathrm{d}}}{\partial t}+\frac{\partial}{\partial x_i}\left(\rho_{\mathrm{d}} u_i\right)=0\,, \tag{1}$$

where ρ_{d} is the symbol of density, u_i is the velocity.

Navier-Stokes equations (2) express Newton's theorem applied to the change of momentum in the form

$$\frac{\partial\left(\rho_{\mathrm{d}} u_i\right)}{\partial t}+\frac{\partial}{\partial x_j}\left(\rho_{\mathrm{d}} u_i u_j\right)+\frac{\partial p}{\partial x_i}=\frac{\partial}{\partial x_j}\left(\tau_{ij}+\tau_{ij}^R\right)+S_i\,, \tag{2}$$

where p is the symbol of pressure, τ_{ij} is the viscous stress tensor.

Energy equation (3) expresses the law of conservation of energy for compressible fluid and it takes the form

$$\frac{\partial \rho_{\mathrm{d}} E}{\partial t}+\frac{\partial\, \rho_{\mathrm{d}} u_i}{\partial x_i}(E+p)=\frac{\partial}{\partial x_i}\left[u_j\left(\tau_{ij}+\tau_{ij}^R\right)+q_i\right]+\tau_{ij}^R\frac{\partial u_i}{\partial x_j}+\rho_{\mathrm{d}}\varepsilon+S_i u_i+Q_{\mathrm{H}}\,. \tag{3}$$

The equation of state (4) for the considered ideal gas is as follows:

$$\rho_{\mathrm{d}}=\frac{pM}{RT}\,. \tag{4}$$

In the above mentioned equations u_i is the fluid velocity, p is the fluid pressure, ρ_{d} the fluid density, M the molar mass of the fluid, T the temperature of the fluid, E the internal energy, S_i the external mass forces (gravity, centrifugal), Q_{H} the supply and heat dissipation per volume unit, q_i the flow heat, τ_{ij} the viscous stress tensor and indexes $_{ij}$ indicate summation variables in three directions according to the coordinates (Einstein summation) [7].

3. The Mathematical-Physical Model

The forces acting on a moving electric charge in an electromagnetic field can be expressed by the specific Lorentz force according to relation [8]

$$\boldsymbol{f}_e=\rho\left(\boldsymbol{E}+\boldsymbol{v}\times\boldsymbol{B}\right), \tag{5}$$

where $\boldsymbol{B}$ is the magnetic flux density vector in the space of a moving electrically charged particle with the volume charge density ρ, $\boldsymbol{v}$ is the mean velocity of the particle, and $\boldsymbol{E}$ is the electric intensity vector [9]. Then, the specific force acting on the moving of electrically charged particles with charge q_e and number N_e and – in the monitored area – with volume V is

$$\boldsymbol{f}_e = \frac{\mathrm{d}\left(N_e q_e\right)}{\mathrm{d}V}\left(\boldsymbol{E} + \boldsymbol{v} \times \boldsymbol{B}\right). \tag{6}$$

On the moving particle in the system A', the relativity effect from the place of the observer system A must still be applied. The model (6) includes this effect. In the example provided by reference [10], current density in the A system is $\boldsymbol{J} = \rho\,\boldsymbol{v}$, for mutually moving Cartesian coordinate system A-A' in the component form [11]

$$\boldsymbol{J}_{\square} = J'_x \mathbf{u}_x + J'_y \mathbf{u}_y + J'_z \mathbf{u}_z + jc\rho' \mathbf{u}_t, \tag{7}$$

where $\boldsymbol{J}$ is the current density 4-vector, $J'_{x,y,z}$ are its components in the Cartesian coordinates A', j is a symbol which indicates an imaginary part of the complex variable (in a harmonious state of phase-shifted by $\pi/2$), c is the velocity of light and ρ' is the volume density of electric charge in the system A'.

The continuity equation can be formulated as follows

$$\operatorname{div} \boldsymbol{J}_{\square} = -\frac{\partial \rho}{\partial t}. \tag{8}$$

After applying the Lorentz transformation to simplify the moving systems in the direction of x, current density (7) can be written in the form

$$\boldsymbol{J}_{\square} = \frac{J'_x + j\frac{v_x}{c} J'_t}{\sqrt{1-\left(\frac{v}{c}\right)^2}} \mathbf{u}_x + J'_y \mathbf{u}_y + J'_z \mathbf{u}_z + j\frac{c\rho' - \frac{v_x}{c} J'_x}{\sqrt{1-\left(\frac{v}{c}\right)^2}} \mathbf{u}_t, \tag{9}$$

where v is the instantaneous particle velocity module (system A) and v_x is its component in the direction of the x axis. To eliminate possible errors in the non-dynamic system of Maxwell reduced equations, it is suitable to include the term which respects Faraday's law of induction [11]

$$\operatorname{rot} \boldsymbol{E} = -\frac{\partial \boldsymbol{B}}{\partial t} + \operatorname{rot}\left(\boldsymbol{v} \times \boldsymbol{B}\right), \tag{10}$$

and for the magnetic field relation (10)

$$\operatorname{rot} \boldsymbol{H} = \boldsymbol{J} + \frac{\partial \boldsymbol{D}}{\partial t} + \operatorname{rot}\left(\boldsymbol{v} \times \boldsymbol{D}\right), \tag{11}$$

The complete Maxwell equations are covariant in all systems, therefore it is not important to specify the system within which the observer moves, because the described relations always hold true. After the derivation of the four-vector and respecting the Lorentz transformation [12], for the moving electric charge with density ρ from the viewpoint of two individual systems relatively moving at the velocity $\boldsymbol{v}$ of A and A', the source current density is written in the form

$$\boldsymbol{J}_{\square} = \rho \frac{\partial \boldsymbol{s}}{\partial t} + jc\rho \mathbf{u}_t, \tag{12}$$

where $\boldsymbol{s}$ is the position vector of a material point in the coordinate system A. Then equation (5) or (6) for the specific force acting on an elementary particle with an electric charge q_e and current density $\boldsymbol{J} = N_e q_e \boldsymbol{v}$ is

$$\boldsymbol{f}_e = \boldsymbol{J}\boldsymbol{v}^{-1}\left(\boldsymbol{E} + \boldsymbol{v}\times\boldsymbol{B}\right) \tag{13}$$

with respect to relative movement systems A-A' the specific power is (14)

$$\boldsymbol{f}_e = \left(\rho\frac{\partial \boldsymbol{s}}{\partial t} + jc\rho\mathbf{u}_t\right)\boldsymbol{v}^{-1}\left(\boldsymbol{E} + \boldsymbol{v}\times\boldsymbol{B}\right). \tag{14}$$

The total specific force acting on the moving electrically charged particles with respect to the velocity of moving electrically charged particles $\boldsymbol{v}$ in the magnetic field is:

$$\boldsymbol{f}_e = \left[\frac{\mathrm{d}\left(N_e q_e\right)}{\mathrm{d}V}\frac{\partial \boldsymbol{s}}{\partial t} + jc\frac{\mathrm{d}\left(N_e q_e\right)}{\mathrm{d}V}\mathbf{u}_t - \frac{\partial\left(\varepsilon \boldsymbol{E}\right)}{\partial t} + \mathrm{rot}\left(\boldsymbol{v}\times\boldsymbol{D}\right)\right]\boldsymbol{v}^{-1}\left[\boldsymbol{E} + \frac{1}{N_e q_e}\left(\frac{m\,\mathrm{d}\boldsymbol{v}}{\mathrm{d}t} + l\boldsymbol{v} + k\int_T \boldsymbol{v}\,\mathrm{d}t\right)\right] +$$
$$+\left[\frac{\mathrm{d}\left(N_e q_e\right)}{\mathrm{d}V}\frac{\partial \boldsymbol{s}}{\partial t} + jc\frac{\mathrm{d}\left(N_e q_e\right)}{\mathrm{d}V}\mathbf{u}_t - \frac{\partial\left(\varepsilon \boldsymbol{E}\right)}{\partial t} + \mathrm{rot}\left(\boldsymbol{v}\times\boldsymbol{D}\right)\right]\times\boldsymbol{B}, \tag{15}$$

where m is the particle mass which is given by the relation

$$m = \frac{m_0}{\sqrt{1 - \dfrac{v^2}{c^2}}}. \tag{16}$$

Further q_e is the electric charge of the moving particle, l is the damping coefficient, and k is the coefficient of stiffness of the ambient environment. Material relations for the macroscopic part of the model are represented by the expressions

$$\boldsymbol{B} = \mu_0\mu_r\boldsymbol{H} \tag{17}$$

and

$$\boldsymbol{D} = \varepsilon_0\varepsilon_r\boldsymbol{E}, \tag{18}$$

where the indexes of quantities of permeabilities and permittivities r denote the quantity of the relative value and the 0 value of quantity for vacuum. By applying the Galerkin method to find the functional minimum and respecting the boundary conditions, the numerical model is obtained as a system of non-linear equations. It will be possible to solve the system of equations using standard methods.

The description of the coupled model with macroscopic properties is perceived in area Ω_F with the pressure parameters which express a body balance (5) [11]

$$\mathrm{div}\overline{T} + \boldsymbol{f} = \frac{\partial\left(\rho_d \boldsymbol{v}\right)}{\partial t} \quad \text{in the area } \Omega_F, \tag{19}$$

where ρ_d is the fluid density and $\boldsymbol{v}$ is the vector of instantaneous velocity. Stress tensor of the relationship (19) can be written as follows (generalized Hooke's law)

$$\overline{T} = \overline{\overline{D}}_F \cdot \overline{e}. \tag{20}$$

Specific deformation tensor is expressed in the form

$$\bar{e} = \begin{bmatrix} \frac{\partial s_x}{\partial x} & \frac{\partial s_x}{\partial y} - \frac{\partial s_y}{\partial x} & \frac{\partial s_x}{\partial z} - \frac{\partial s_z}{\partial x} \\ \frac{\partial s_x}{\partial y} - \frac{\partial s_y}{\partial x} & \frac{\partial s_y}{\partial y} & \frac{\partial s_y}{\partial z} - \frac{\partial s_z}{\partial y} \\ \frac{\partial s_x}{\partial z} - \frac{\partial s_z}{\partial x} & \frac{\partial s_y}{\partial z} - \frac{\partial s_z}{\partial y} & \frac{\partial s_z}{\partial z} \end{bmatrix} \tag{21}$$

Putting the stress tensor (20) and power density (15) into equation (19) and itemizing this equation we obtain

$$(\lambda_1 + \lambda_2)\text{grad div}\mathbf{s} + \lambda_2 \nabla^2 \mathbf{s} + \mathbf{f}_s = \frac{\partial(\rho_\text{d}\mathbf{v})}{\partial t} \tag{22}$$

where λ_1, λ_2 are

$$\lambda_1 = \frac{E_\text{u}\sigma}{(1+\sigma)(1-2\sigma)} \tag{23}$$

and

$$\lambda_2 = \frac{E_u}{2(1+\sigma)}. \tag{24}$$

For Poisson ratio σ applies $\sigma \neq -1 \wedge \sigma \neq 0.5$.

This work does not deal with particle trajectories; however, it is focused on the evaluation of the pressure gradient in a small nozzle area. Then it is possible to linearize this model piecewise.

4. Finite Element/Volume Method

The finite volume method is a discretization method which is well suited for the numerical simulation of various types of conservation laws. It has been extensively used in several engineering fields, such as fluid mechanics, heat and mass transfer or petroleum engineering. Some of the important features of the finite volume method are similar to those of the finite element method. The method may be used on arbitrary geometries, using structured or unstructured meshes, and it leads to robust schemes.

The finite volume method is a numerical method for solving partial differential equations that calculates the values of the conserved variables averaged across the volume. One advantage of the finite volume method over finite difference methods is that it does not require a structured mesh (although a structured mesh can also be used). Furthermore, the finite volume method is preferable to other methods as a result of the fact that boundary conditions can be applied noninvasively. This is true because the values of the conserved variables are located within the volume element, and not at nodes or surfaces. Finite volume methods are especially powerful on coarse non-uniform grids and in calculations where the mesh moves to track interfaces or shocks [13-15]. The method is used in many computational fluid dynamics packages [16].

A supersonic flow created by apertures with circular orifices is accompanied by a local reduction in pressure (Fig. 3). This is an advantage in relation to the scattering of secondary electrons. There is a slight local decrease in pressure. Some energy is lost to the free expansion of gas around the nozzle mouth due to its geometry (Figs 4 and 5).

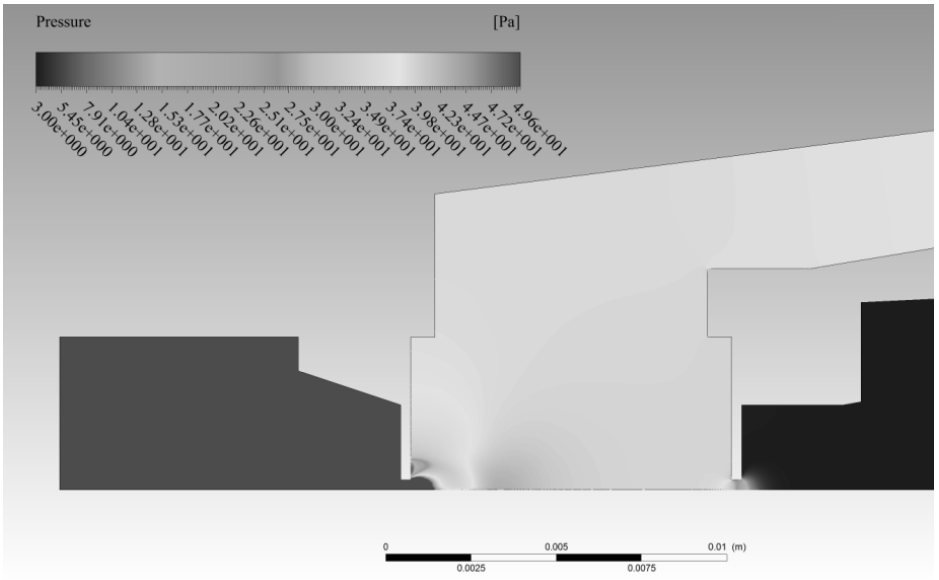

Fig. 3 The pressure as it passes through the first aperture (circular orifice)

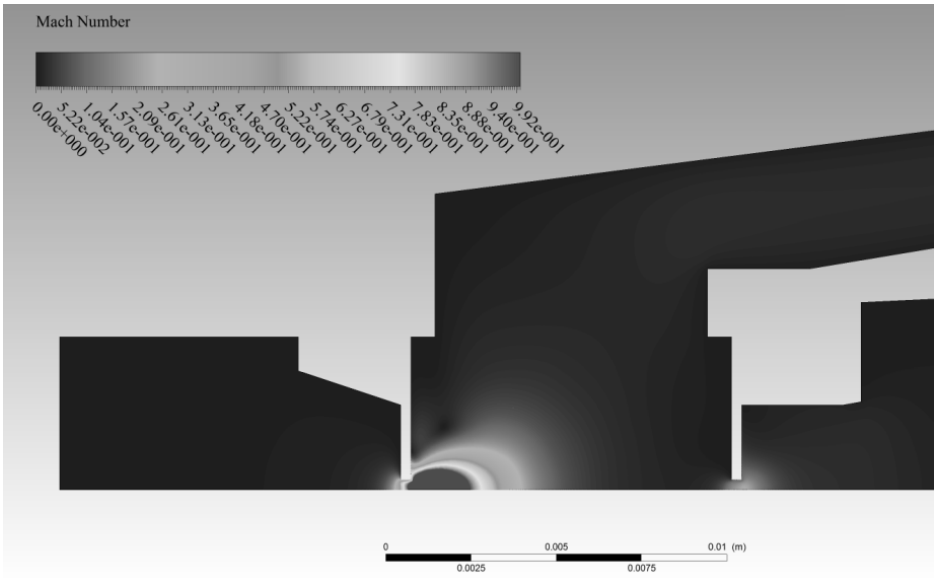

Fig. 4 The Mach number as it passes through the first aperture (circular orifice)

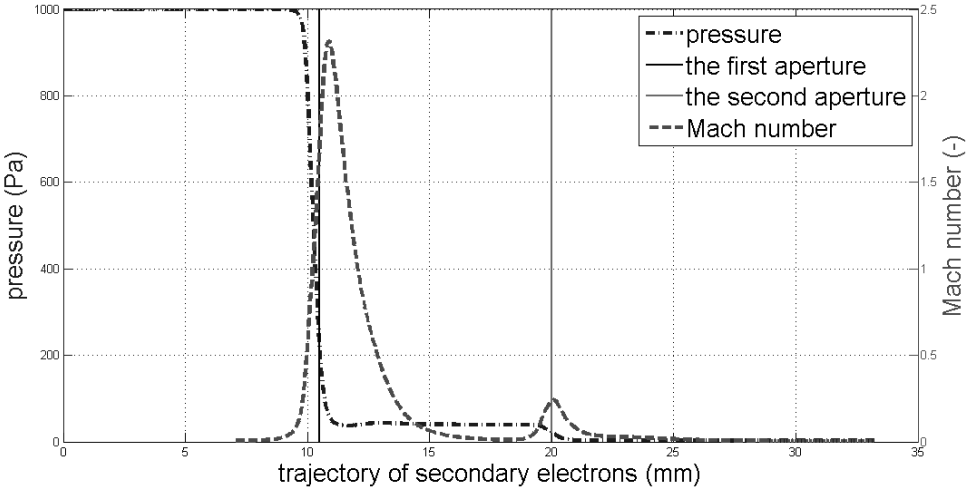

Fig. 5 Pressure profile and Mach number in apertures with circular orifice

The energy lost in uncontrolled expansion allows the use of the Laval nozzle, which consists of a convergent part (tapers to a critical section) and divergent part, which directs the gas expansion to the critical cross section (Fig. 6). In the convergent part the gas reaches the critical speed and in the divergent part the gas is further accelerated (Fig. 7).

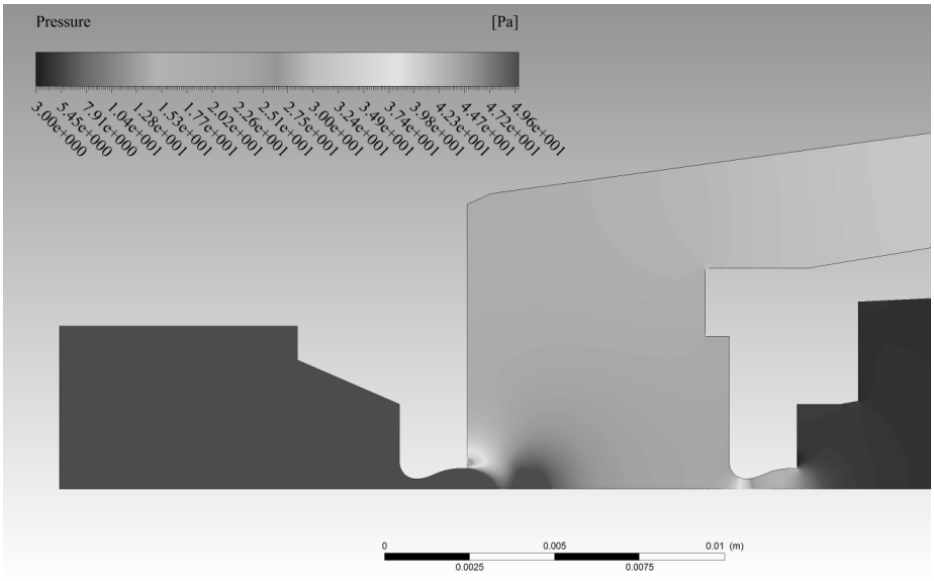

Fig. 6 The pressure as it passes through the first aperture (Laval nozzle)

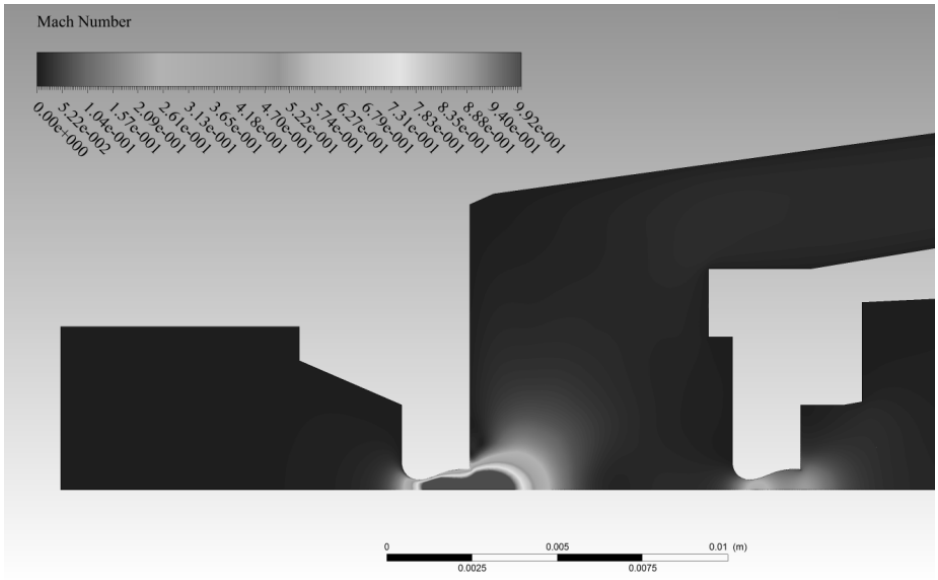

Fig. 7 The Mach number as it passes through the first aperture (Laval nozzle)

The characteristic feature of the Laval nozzle is called a double expansion wave, which can be used to streamline the passage of the secondary electrons through the detector at a higher pressure in the specimen chamber (Fig. 8). Double expansion wave extends the area of low pressure. This affects the media pressure conditions entering into the second aperture and thus the pressure at the scintillator.

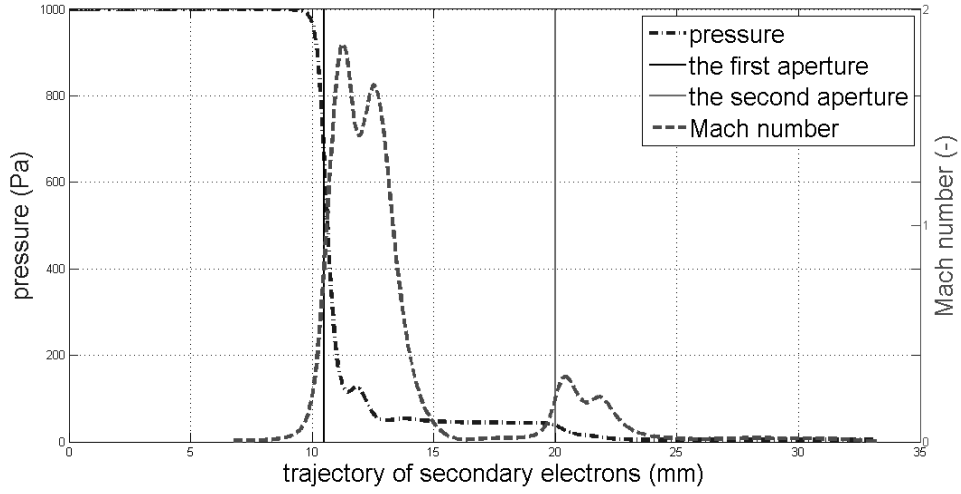

Fig. 8 Pressure profile and Mach number in apertures with Laval nozzle.

5. Discussion

The supersonic flow through the aperture can cause shock waves. This is a significant compression of gas at short distances, which may create a barrier to the passage of electrons. The shock wave is a step change value (pressure, density), and it creates a discontinuity which in the calculations by the finite volume method cannot be described without a correct approximation type. The second order upwind method was used to investigate shock waves. Figures 3, 4, 6, and 7 show us the pressure compression behind the aperture. It assumes that shock waves can occur in these places.

6. Conclusion

When setting up pressures in the range of 200 to 1000 Pa at the inlet of the scintillator, the results show that at the Laval nozzle pressure drops faster than at an aperture with a circular orifice. Due to the requirement to maintain the pressure on a lower trajectory of secondary electrons in the scintillator chamber, the aperture with the Laval nozzle appears to be better.

Aperture C1 determines the pressure ratios across the detector. Gas that enters into it is moving into a critical state and moves at supersonic speed. Gas entering into aperture C2 is already moving at subsonic speeds, far below the Mach number. In some cases, swirls are formed directly in apertures or even before the entry into the first aperture, which again affects the pressure in the detector.

References

[1] JIRÁK, J., NEDĚLA, V., ČERNOCH, P., ČUDEK, P. and RUNŠTUK, J. Scintillation SE detector for variable pressure scanning electron microscopes. *Journal of Microscopy*, 2010, vol. 239, no. 3, p. 233-238. DOI: 10.1111/j.1365-2818.2010.03377.x.

[2] DANILATOS, G. Design and construction of an atmospheric or environmental SEM (part 3). *Scanning*, 1985, vol. 7, no. 1, p. 26-42. DOI: 10.1002/sca.4950070102.

[3] DANILATOS, G. Velocity and ejector-jet assisted differential pumping: Novel design stages for environmental SEM. *Micron*, 2012, vol. 43, no. 5, p. 600-611. DOI:10.1016/j.micron.2011.10.023.

[4] MAXA, J., NEDĚLA, V., JIRÁK, J., VYROUBAL, P. and HLADKÁ, K. Analysis of Gas Flow in a Secondary Electron Scintillation Detector for ESEM with a new system of Pressure limiting Apertures. *Advances in Military Technology*, 2012, vol. 7, no. 2, p. 39-44. ISSN 1802-2308.

[5] MAXA, J., NEDĚLA, V. and JIRÁK, J. Analysis of Gas Flow in the new system of Apertures in the Secondary Electron Scintillation Detector for ESEM. *Microscopy and Microanalysis*, 2012, vol. 18, supplement 2, p.1264-65. ISSN 1431-9276.

[6] VERSTEEG, K. and MALALASEKERA, W. *An Introduction to Computational Fluid Dynamics: The Finite Volume Method*. Reading, Addison-Wesley, 1995. 257 p.

[7] VYROUBAL, P. and MAXA, J. Analysis of the Impact of Supersonic Flow in Detector of Secondary Electrons ESEM. In *Proceedings 2nd Computer Science On-Line Conference*. Ithaca: Cornell University 2012, p. 149-155.

[8] FIALA, P. Pulse-powered virtual cathode oscillator. *Transactions on Dielectrics and Electrical Insulation*, 2011, vol. 18, no. 4, p. 1046-1053. ISSN 1070-9878.

[9] BAČA, P. Possibilities of electric power storage from renewable sources. *Acta Montanistica Slovaca*, 2010, vol. 15, special issue no, 2, p. 100-104. ISSN1335-1788.

[10] FIALA, P., FRIEDL, M. and SZABÓ, Z. EMHD Models Respecting Relativistic Processes of Trivial Geometries. *Progress in Electromagnetics*, 2011, vol. 2011, p. 96-99. ISSN 1559- 9450.

[11] STRATTON, JA. *Electromagnetic Theory*. New York: Mc Graw-Hill, 1941. 630 p.

[12] KIKUCHI, H. *Electrohydrodynamics in dusty and dirty plasmas, gravito-electrohydrodynamics and EHD*. Kluwer Academic Publishers, 2001, 228 p.

[13] MAXA, J. and NEDĚLA, V. Impact of the critical Flow on Conditions of the Primary Electron Beam passage through the Differentially Pumped Chamber. *Advances in Military Technology*, 2011, vol. 6, no. 1, p. 39-47. ISSN 1802-2308.

[14] HYMAN, M. and KNAPP, R. High Order Finite Volume Approximations of Differential Operators on Nonuniform Grids. *Physica D: Nonlinear Phenomena*, 1992, vol. 60, no. 1-4, p. 112-138. ISSN 0167-2789.

[15] RÜBENKÖNIG, O. *The Finite Volume Method (FVM)*. [cited 2012-12-12]. Available from: <www.imtek.uni-freiburg.de/simulation/mathematica/imsReferencePointers/FVM_introDocu.htm>

[16] MAXA, J., VYROUBAL, P., VANĚK, J. and SOLČANSKÝ, M. The finite volume method in photovoltaic – The cooling system of concentrator solar panels. *ECS Transactions*, 2013. ISSN 1938-6737 (in print).

Acknowledgement

This work was supported by the EU project No. CZ.1.05/2.1.00/01.0014, project FEKT-S-11-7 and Czech Science Foundation: grant No. GAP 102/10/1410.